Brain Tumor Detection Based on Amended Convolution Neural Network Using MRI Images

Mohanasundari M[1*], Dr. Chandrasekaran V[2], and Dr. Anitha S[3]
[1*]Department of Computer Science and Engineering, Velalar College of Engineering and Technology, Erode – 638012, Tamilnadu, India
[e-mail: msmohana86@gmail.com]
[2]Department of Electronics & Communication Engineering, Velalar College of Engineering and Technology, Erode – 638012, Tamilnadu, India,
[e-mail: vcresearch@gmail.com]
[3]Department of Information Technology, Kongu Engineering College, Perundurai, Erode-638 060, Tamilnadu, India
[e-mail: anithame@kongu.ac.in]
[*]Corresponding author: Mohanasundari M

Received February 8, 2023; revised May 11, 2023; revised July 4, 2023; revised August 5, 2023; accepted September 19, 2023; published October 31, 2023

Abstract

Brain tumors are one of the most threatening malignancies for humans. Misdiagnosis of brain tumors can result in false medical intervention, which ultimately reduces a patient's chance of survival. Manual identification and segmentation of brain tumors from Magnetic Resonance Imaging (MRI) scans can be difficult and error-prone because of the great range of tumor tissues that exist in various individuals and the similarity of normal tissues. To overcome this limitation, the Amended Convolutional Neural Network (ACNN) model has been introduced, a unique combination of three techniques that have not been previously explored for brain tumor detection. The three techniques integrated into the ACNN model are image tissue pre-processing using the Kalman Bucy Smoothing Filter to remove noisy pixels from the input, image tissue segmentation using the Isotonic Regressive Image Tissue Segmentation Process, and feature extraction using the Marr Wavelet Transformation. The extracted features are compared with the testing features using a sigmoid activation function in the output layer. The experimental findings show that the suggested model outperforms existing techniques concerning accuracy, precision, sensitivity, dice score, Jaccard index, specificity, Positive Predictive Value, Hausdorff distance, recall, and F1 score. The proposed ACNN model achieved a maximum accuracy of 98.8%, which is higher than other existing models, according to the experimental results.

Keywords: Brain tumor, CNN, Image tissue feature extraction, Medical science, Magnetic Resonance Imaging, Marr Wavelet Transformation, Sigmoid activation function

1. Introduction

The brain tumor is considered the deadliest disease. A Nature-inspired Resnet-152 model, integrated with a Deep Convolutional Neural Network (CNN), was proposed in [1] for the classification of brain images. In [2], an innovative approach called the Border Collie Firefly Algorithm along with a Generative Adversarial Network (BCFA-based GAN) was introduced. This approach utilized the spark framework to facilitate brain tumor classification. However, the precision was not improved by BCFA-based GAN. The segmentation was carried out in [3] with a swarm-based grasshopper optimization algorithm (SGHO). However, the segmentation time was not reduced by SGHO. The dark-nets model has been suggested in reference [4] for the aim of categorizing, locating, and splitting brain tumors by utilizing MRI. An automatic mechanism was introduced in [5] to perform tumor classification with MRI images. The pre-processing was carried out to normalize the intensity whereas the segmentation was carried out with the Optimal DeepMRSeg strategy which is said to be known as a deep learning-based segmentation method. However, the recall was not improved by using an automatic mechanism. In [6], researchers introduced Artificial Neural Networks (ANN) to classify MRI images of brain tumors. Furthermore, in [7], a novel classification technique was proposed for distinguishing MRI brain tumors from human brain images. Pre-processing, Segmentation, and Feature extraction processes were carried out for MRI classification. However, the classification time was not reduced by the classification technique.

A brain tumor classification method was introduced in [8] with a fusion of deep and shallow features but, the level of accuracy was not improved by the designed method. Hence, the Deep Neural Networks (DNN) based Visual Geometry Group (VGG-16) network was introduced in [9] to increase the level of accuracy. For classification, a deep learning method has been introduced [10]. But, the F1-score was not improved by Enhanced Faster Region-Based CNN (R-CNN). To overcome this issue in the existing research models, a new approach called the Amended Convolutional Neural Network (ACNN) has been introduced which is a unique combination that has not been previously explored for brain tumor detection. The combination of three separate methodologies in this methodology improves the accuracy as well as reliability of brain tumor identification.

The contributions of this work are:

- To improve the accuracy of automated brain tumor detection, a newly proposed deep learning model called ACNN has been introduced. This model is based on CNN and is designed to perform preprocessing, segmentation, and feature extraction tasks.
- To eliminate noisy pixels in the image tissues, Kalman Bucy (KB) Smoothening Filters are utilized as they are capable of providing accurate estimates of the underlying images and being able to adapt to varying conditions.
- To handle low-contrast images and for a more precise segmentation of pre-processed images into multiple segments, the Isotonic Regressive Image Tissue technique was used.
- For extracting the image tissue features, Marr Wavelet Transformation was utilized for extracting the features in the MRI images and also for detecting the tumor in multiscale in different resolutions with fast computation.
- The sigmoid activation function matches testing features with extracted features. Eventually, it enhanced the identification of tumor cells more accurately and it automatically made the ACNN model more efficient in the prediction process.

- The proposed model's effectiveness is evaluated using several metrics such as specificity, F1-score, accuracy, loss, confusion matrix, ROC, dice score, Jaccard index, testing time, precision, recall, PPV, FPV, MAE, and Hausdorff distance and found to be better the state-of-the-art existing systems.

The road map is given: Section 2 reviews the related articles on brain tumor detection. Section 3 provides a comprehensive examination of the proposed ACNN model, accompanied by a well-organized architecture diagram. In Section 4, the experimental settings are outlined, including detailed descriptions of the datasets used. Section 5 performs the result discussion with the existing methods and the conclusion is given in Section 6.

2. Literature Review

For categorizing brain tumors, an ensemble learning method has been used [11] but, the computational cost was high and not reduced. Classification of brain tumors depending on Artificial Intelligence has been introduced in [12] for classifying brain tumor images but, AI-based classification hasn't improved the precision level. An intelligent method was introduced in [13] for tumor detection. The fuzzy centroid-based region was employed for image segmentation. But the recall was not improved by the designed method.

A unique approach was introduced in [14] for detecting and classifying MR brain images. In this approach, the noise was effectively eliminated by applying a Gaussian filter. Subsequently, a range of image features including embedded, cyclic, contrast, and block appearance were extracted to facilitate the segmentation process. A cross-validation approach was used in combination with a Support Vector Machine (SVM) to perform classification. The classification of brain tumors was achieved using Bayesian fuzzy clustering as reported in [15]. However, it should be noted that the computational complexity of the brain tumor classification was not reduced.

CNN algorithm was designed in [16] to partition the brain tumor. CNN algorithm, however, has not improved the F1-measure. CNN was established in [17] to enhance the grading and classification of brain tumors. In [18], a six-layer deep CNN was employed to classify brain images obtained from MRIs into four distinct classes. For improving data augmentation and detecting brain tumors, an efficient method based on CNN was introduced using MRI datasets [19]. A tumor detection method was introduced in [20] depending on saliency modeling. A new strategy was introduced in [21] to extract the brain tumor. A suggested technique for the categorization of MRI brain images has been presented in [22], utilizing several wavelet transforms such as Discrete Wavelet Transform (DWT) and Stationary Wavelet Transform (SWT) to obtain enhanced efficiency.

To recognize brain tumors on MRI images, a new approach was introduced in [23]. Though this system has assisted doctors in diagnosing various dangerous diseases in humans it has not improved the recall. A segmentation and detection method was designed in [24] for brain tumors to identify the tumor area.

Nevertheless, the designed segmentation and detection method did not result in a reduction in time complexity. In [25], a framework based on blockchain was suggested, employing Hyperledger Fabric along with adaptable access control policies, and this proposed framework made use of a cross-domain framework.

In [26], a new algorithm called Binary Spring Search (BSS), based on Group Theory (GT), was presented. This algorithm utilized a combination of deep neural networks and aimed to enhance security, efficiency, and transparency while remaining cost-effective in handling

healthcare data. Current blockchain-based healthcare schemes provide merely a framework for data exchange and lack adequate safety and confidentiality safeguards. As a result, [27] proposed a lightweight authorization and data retention system for Cyber-Physical Systems (CPS) built around the Internet of Medical Things (IoMT). The suggested approach attempted to alleviate these issues by providing decentralized authentication among approved devices.

In 2021, a brain tumor detection method was proposed that demonstrated high sensitivity and specificity [28]. However, the limitation of this study was set to use only a small dataset which may not represent the entire population. In 2022, two deep learning models were proposed for identifying binary and multiclass brain tumors, but the limited amount of accurately annotated data was still a challenge [29]. In different research, a method for automated detection of brain tumors was put forth. This method utilized variations of Local Binary Pattern (LBP) based on empirical wavelet transform, along with ant-lion optimization. The study demonstrated encouraging outcomes; however, it should be noted that the method lacked external validation and clinical evaluation [30]. Similarly, a diagnostic system was proposed using the Fractional Wavelet Transform (FWT) for brain tumor detection with MRI, but the study's limitations included a small dataset and a lack of external validation [31]. A suggestion for a technique that uses ensemble deep learning frameworks and Class Activation Maps (CAMs) markers to diagnose brain cancers using MRI images was provided in [32].

The study collection includes a wide spectrum of research on the recognition and categorization of brain tumors using various approaches. While these works contribute to the field, they also have certain limitations. For example, some of the studies relied on traditional machine learning algorithms like SVM [3] or feature selection techniques [6], which may not fully leverage the power of deep learning models.

Other works utilize specific architectures like CNN [14, 21] or autoencoders [15], but they may not explore the potential of more advanced architectures like GANs [5] or ensemble learning [11]. Additionally, some of the studies were focusing solely on tumor detection [20, 23], while others were focusing on classification [10, 17]. Additionally, some studies encounter drawbacks such as limited dataset sizes, absence of external validation, significant computational burdens, and an inability to enhance precision.

Compared to the previous studies, the objective of this paper is to overcome the drawbacks and enhance the existing methods by introducing a unique hybrid deep learning model for the recognition and categorization of brain tumors. In this work, binary classification of brain tumors from MRI images has been performed. This hybrid approach allows for better feature representation and generalization capabilities compared to using traditional machine learning algorithms alone. In addition, if accuracy, precision, recall, and other relevant assessment criteria are considered, the proposed ACNN model outperforms previous approaches. Additionally, incorporating the Marr wavelet for feature extraction from MRI images has the potential to further enhance the accuracy of the model.

3. Methodology

Though the brain tumor is identified using different methods the conventional methods haven't enhanced the level of accuracy. To solve the existing issues, the Amended Convolutional Neural Network (ACNN) model has been introduced, and found that the ACNN Model outperforms brain tumor image tissue classification. The architecture diagram of the ACNN Model is illustrated in **Fig. 1**.

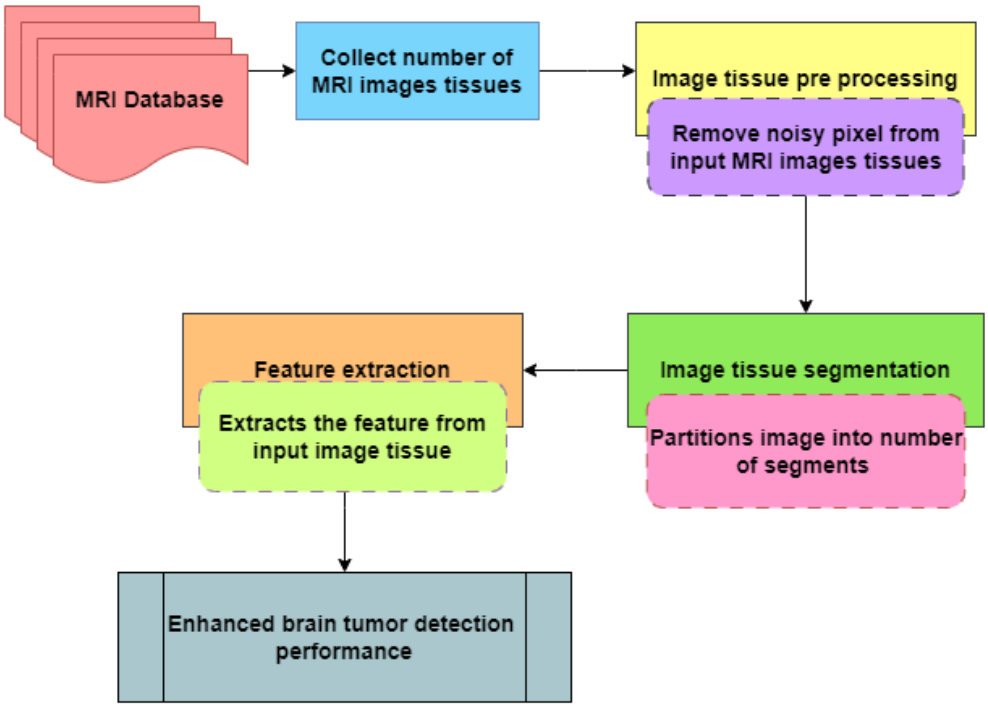

Fig. 1. Architecture Diagram of ACNN Model

The overall architecture diagram of the ACNN model for brain tumor detection is illustrated in **Fig. 1**. The proposed approach is divided into three parts: pre-processing, segmentation, as well as feature extraction. Firstly, the image tissue pre-processing step is responsible for eliminating noisy pixels from the input images. Subsequently, the image tissue segmentation process is performed to divide the image into multiple segments. Next, the image tissue feature extraction step was employed for extracting related features from the segmented regions. Lastly, image categorization is accomplished with greater accuracy using the obtained characteristics. The schematic diagram of the deep convolutional neural network is illustrated in **Fig. 2**. In **Fig. 2** the input layer of the proposed model consists of MRI images. The model comprises three hidden layers, each with a specific function. Hidden layer 1 is responsible for image pre-processing, hidden layer 2 handles image segmentation, and hidden layer 3 performs feature extraction. The output layer produces the outcomes, indicating the detection results for brain tumors.

The input MRI image tissues 'M_{RI_1}, M_{RI_2}, M_{RI_3} ….. M_{RI_n}' are gathered and sent to the input layer from the database and it is formulated as,

$$I(t) = \sum_{i=1}^{n} M_{RI_i} * we_{input} + bias \qquad (1)$$

From (1), 'M_{RI_i}' with initial weight 'we_{input}' is considered. The first process of the proposed ACNN model is to remove the unwanted noisy pixels by using the KB Smoothening Filter in hidden layer 1. This filter is a series of observations taken over time that are estimated by calculating the joint probability distribution across variables for each time frame.

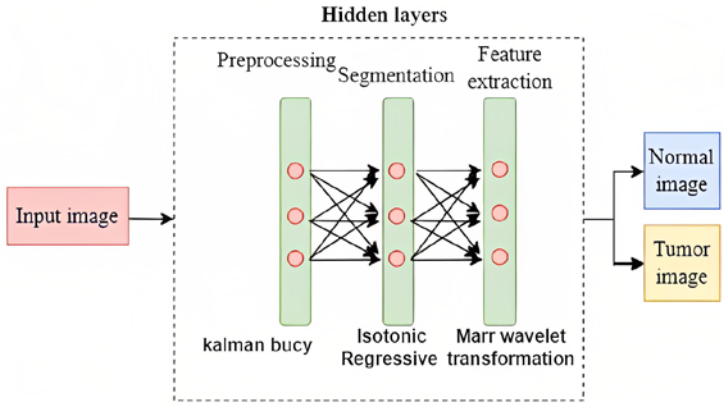

Fig. 2. Schematic Diagram of ACNN Model

KB Smoothening Function in ACNN Model is formulated as,

$$Gf(x) = F_k x_{k-1} + B_k u_k + w_k \tag{2}$$

From (2), 'F_k' and 'B_k' symbolizes the state transition model and control-input model respectively. The hidden layer involves the image tissue segmentation by using Isotonic Regression Analysis. Isotonic Regression analysis is a free-form line to a series of observations where the fitted line is non-decreasing and lies near the observations. The ACNN Model separates the pre-processed image into several segments using its isotonic regressive image tissue segmentation procedure.

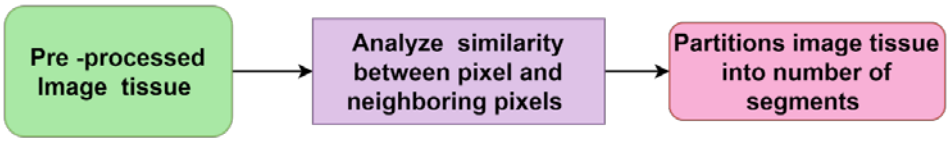

Fig. 3. Isotonic Regressive Image Tissue Segmentation

Fig. 3 describes the isotonic regression analysis. The regression function uses isotonic regression analysis to examine the tissue pixels in the input image whereas the Rogers–Tanimoto Similarity Index in the ACNN Model finds the similarity between pixels. It is calculated as,

$$RTSI = \frac{Pixel_a + Pixel_d}{N + Pixel_b + Pixel_c} \tag{3}$$

From (3), '$RTSI$' denotes the Rogers–Tanimoto similarity index. '$Pixel_a$' represents the image tissue pixels. '$Pixel_b$', '$Pixel_c$', and '$Pixel_d$' represents the closest pixel in an imaged tissue. A similarity value between 0 and 1 is represented by the coefficient ($0 \leq RTSI \leq 1$). In hidden layer 3, feature extraction is performed using Marr Wavelet Transformation. For extracting the features, the segmented image tissues are split into horizontal and vertical directions within different levels. Marr Wavelet Transformation is performed in the ACNN Model and the Marr Wavelet Transformation is the negative normalized second derivative of the Gaussian function. The multidimensional generalization of wavelet is the Laplacian of Gaussian function. The wavelet is approximated through the

Difference in Gaussian (DoG) function. A DoG is separable and saves considerable computation time in two or more dimensions. It is mathematically expressed as,

$$\psi(Pixel_a.Pixel_b) = \frac{1}{\pi\sigma^4}\left(1 - \frac{1}{2}\left(\frac{{Pixel_a}^2+{Pixel_b}^2}{\sigma^2}\right)\right)e^{-\frac{{Pixel_a}^2+{Pixel_b}^2}{2\sigma^2}} \quad (4)$$

From (4), 'σ' denotes the constant, and the hidden layer output is denoted as,

$$H(t) = \sum_{i=1}^{n} M_{RI_i} * we_{input} + [H(t-1) * we_{hh}] \quad (5)$$

The hidden layer output is shown by 'H(t)' in (5). The term 'we_{input}' refers to the weight assigned to input and hidden layers. " $H(t-1)$" denotes the outcome of the former hidden layer. The word 'we_{hh}' represents the weight between two levels that are veiled. Then, the output layer performs image tissue categorization by using the hidden layer results using the sigmoid activation function in the ACNN model. The ACNN Model utilizes the sigmoid activation function to enhance the accuracy of detecting tissue in both training and testing images. It is given by,

$$Sigmoid_{af} = \frac{1}{\sum_{i=1}^{K} 1+e^{-s_i}} \quad (6)$$

From (6), '$Sigmoid_{af}$' denotes the sigmoid activation function. 's_i' denotes the segmented tissue from the image, The output layer of the ACNN Model is represented as,

$$O(t) = we_{oh} * H(t) \quad (7)$$

The symbol " O(t)" represents the result of the output layer as obtained from equation (7), while the notation 'we_{oh}' denotes the weight associated with the connection between the hidden layer and the output layer.

Table 1. ACNN Algorithm for Brain Tumor Detection

Begin
Input: Magnetic Resonance Image Database '$M_{RI_1}, M_{RI_2}, M_{RI_3} \ldots\ldots M_{RI_n}$'
Output: normal and abnormal image classification
Load the input image data
1: Assume $I(t)$ be the input Magnetic Resonance Image Database
2: Initialize magnetic resonance images M_{RI_1}, M_{RI_2}, $M_{RI_3} \ldots\ldots M_{RI_n}$
3: for each M_{RI}
4: Eliminates the noisy pixels through image tissue pre-processing in hidden layer 1 using Kalman Filter
5: Perform the image tissue segmentation process in hidden layer 2 using Isotonic Regressive Image Tissue Segmentation Process.
6: Determine the Rogers–Tanimoto similarity between pixels
7: similarity value coefficient ($0 \leq RTSI \leq 1$)
8: Partition the images
9: Extract the features in the hidden layer 3 using Marr Wavelet Transformation
9: end for
10: For every image tissue
11: Use the sigmoid activation function to test and train the image tissue for detection.
12: if ($Sigmoid_{af} > th$)then

```
13:   output O(t)
14:       Categorized as abnormal
15:    Else
16:       Categorized as normal
17:        End if
18: End for
End
```

Table 1 describes the algorithmic approach to identifying brain tumor diseases in the ACNN Model with more accuracy. By using the output layer classification, brain tumors will be detected within a short period based on the analysis.

4. Dataset Description

In this study, the Brain Tumor MRI dataset [33] was utilized, and sample images of both normal and tumor instances are depicted in **Fig. 4**. The first openly accessible database of brain MRI scan images was made available on the Kaggle website. This database comprises 7023 MRI images in total under two classes namely tumor, and no tumor. This research takes into account 3929 image files with 2556 no tumor and 1373 tumor images. The binary-class classification is applied in this work using the proposed model and these images are pre-processed before being fed to the model.

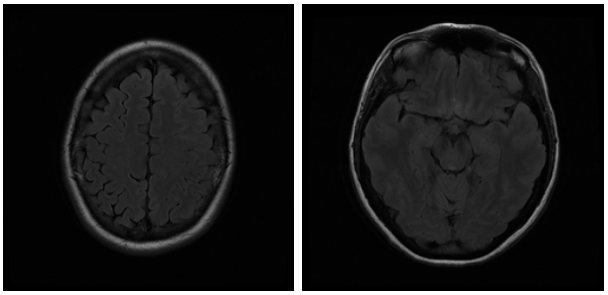

(a) Normal images

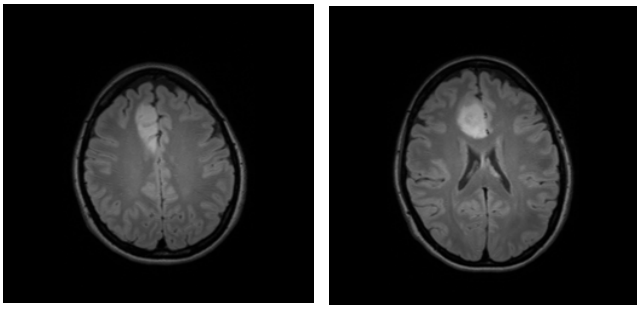

(b) Tumor images

Fig. 4. (a) normal images and (b) tumor images in the brain

5. Results and Discussion

The suggested ACNN Model is described together with two other related approaches that are currently in use: 23 layers CNN [29], Ensemble model [32], Fractional Wavelet [31], and PCA and TK- means [28] by using the various performance metrics like accuracy, sensitivity, dice score, Jaccard index, recall, Positive predictive value, specificity, Hausdorff distance, precision, and F1 score. True Positive (TP), True Negative (TN), False Positive (FP), as well as False Negative (FN) classes can be utilized to compute these measurements. Positive pixels that have been correctly classified are referred to as TP whereas the Positive pixels that have been erroneously identified are referred to as FN. Negative pixels that have been accurately identified are termed as TN whereas the improperly recognized negative pixels are referred to as FP. **Table 2** displays the hyperparameters utilized in the proposed ACNN model.

Table 2. Hyperparameter of the proposed ACNN model

Parameter	**values**
Learning rate	0.0001
Iterations	8
Epochs	14
Batch size	16
optimizer	Adam
Activation function	Sigmoid

5.1 Confusion matrix

The test data are used to construct a confusion matrix, which measures the efficiency of the proposed model. The confusion matrix is generated using true class data and forecasted class data. This matrix has four outcomes: TP, TN, FP, and FN.

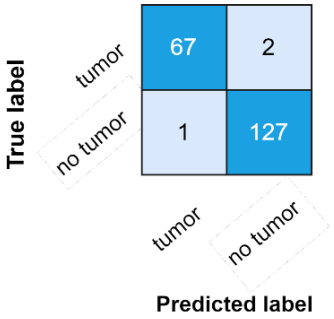

Fig. 5. Confusion matrix for proposed work

The confusion matrix for the proposed model is shown in **Fig. 5**. It signifies the findings of an inquiry on a brain tumor MRI dataset for the classes, tumor, and no tumor. 67 out of 69 glioma tumors are classified as tumors whereas the remaining 2 are classified as no tumors. The accuracy of the model is very high since only a few cases of misclassified data are there.

Table 3. Input and Output Samples of Brain Tumor Detection using ACNN

Input	Feature extraction	Final output/classification
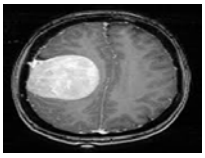	array([0.01176471, 0.01176471, 0.01176471, ..., 0.00392157, 0.00392157, 0.00784314])	yes
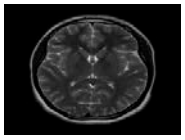	array([0, 0, 0, ..., 0, 0, 0]	no

Two figures representing input images are shown in **Table 3**, one with and one without tumors. The feature extraction block then receives the pre-processed image. A set of numerical values that reflect the extracted features will be produced once the Marr wavelet transform has been applied to the MRI images. The procedure of classification is then carried out, with two classes being used: tumor and no tumor. The accuracy level represents the proportion of patient records that are correctly classified as having a specific condition or not, and it is calculated as follows:

$$Acc_L = \left(\frac{PD_{tp}+PD_{tn}}{N}\right) * 100 \tag{8}$$

From (8), 'Acc_L'represents the accuracy level. 'PD_{tp}' denotes the true positive. 'PD_{tn}' symbolizes the true negative. N stands for the number of MRI images used. The accuracy rating is expressed as a percentage (%).

Precision is determined depending on the true positives and false negatives of patient data and it is calculated as,

$$P_{re} = \left(\frac{PD_{tp}}{PD_{tp}+PD_{fp}}\right) * 100 \tag{9}$$

From (9), 'P_{re}' denotes the precision. 'PD_{fp}' denotes the false positive and 'PD_{fn}' indicates the false negative. Recall, in the context of brain tumor disease classification, is used to identify the number of true positives and false negatives. It is computed as,

$$Re_{call} = \left(\frac{PD_{tp}}{PD_{tp}+PD_{fn}}\right) * 100 \tag{10}$$

From (11), The specificity of a classifier can be defined as the proportion of the amount that was correctly identified as negative to the genuinely negative amount. The F1 score is regarded to be a stronger predictor of classifier performance than the standard accuracy measure as stated in equation (12),

$$specificity = \frac{TN}{FP+TN} \quad (11)$$

$$F1 - score = \frac{2 * Precision * Recall}{Precision + Recall} \quad (12)$$

Positive predictive value: The TP also displays the likelihood that a given set of pixels was accurately classified.

$$Positive\ predictive\ value = \frac{TP}{TP+FP} \quad (13)$$

Table 4. Performance comparison of the proposed model with the existing algorithm

Parameters	**Proposed algorithm**	**Existing algorithm**			
	Amended convolution	**23 layers CNN** [29]	**Ensemble model** [32]	**Fractional Wavelet** [31]	**PCA and TK-means** [28]
Accuracy	98.8	96.7	93.45	92.13	91.5
F1 score	0.918	0.904	0.892	0.884	0.863
Precision	0.894	0.885	0.871	0.867	0.852
Recall	0.944	0.924	0.913	0.894	0.879
Specificity	89.47	87.23	85.67	84.53	83.22
Sensitivity	90.90	88.12	87.26	86.34	85.74
Positive predictive value	89.33	86.34	85.23	84.22	83.67

Table 4 demonstrates that the modified convolution method proposed for brain tumor detection attained an accuracy of 98.8%, surpassing the accuracy, F1 score, precision, recall, and positive predictive value of all existing algorithms. In comparison, the existing 23-layer CNN network achieves an accuracy of 96.7% which is significantly lower than the proposed algorithm. This is because the 23-layer CNN network [29] relies solely on convolutional layers for feature extraction without any additional pre-processing techniques.

Although the network is deep and may capture more complex features, it may not be effective in removing noise from input images, which may affect the accuracy of the classification. The existing ensemble model [32] achieves an accuracy of 93.45%, which is lower than both the proposed and the 23-layer CNN network. Though the ensemble model combines multiple models, it may not be efficient in handling highly complex data with multiple features. The existing PCA and TK-means [28] approach and the fractional wavelet [31] achieve an accuracy of 91.5% and 92.3%which is lower than all other existing and proposed algorithms. These two methods work better when the number of datasets is limited, but their performance is affected by this limitation and it reduces their classification accuracy.

The proposed ACNN utilizes a large MRI image dataset with advanced image processing techniques such as KB Smoothing Filter, Isotonic Regressive Image Tissue Segmentation, and Marr Wavelet Transformation for feature extraction. It was found that the proposed algorithm for brain tumor detection outperforms all the other existing algorithms in terms of accuracy and other performance metrics. The Dice score and Jaccard index are also commonly used metrics for evaluating the segmentation tasks in medical imaging. The Dice score is utilized to determine the level of similarity between the two sets namely M and N and it is expressed as,

$$Dice\ score = \frac{2\times|M\cap N|}{|M|+|N|} \tag{14}$$

In equation (14), |M| and |N| represent the cardinalities for sets M and N accordingly.

The intersection of two sets divided by their union is denoted as the Jaccard index between them. The Jaccard Index compares two images based on their similarities and differences.

$$Jaccard\ index\ = \frac{|M\cap N|}{|M\cup N|} \tag{15}$$

The Hausdorff distance (HD) is utilized to measure the separation or dissimilarity between the ground truth contour A and the segmented contour B. The segmentation method achieves optimal segmentation outcomes when the HD value approaches zero.

$$HD = \max\big(h(A,B), h(B,A)\big) \tag{16}$$

Table 5. Performance comparison of existing and proposed algorithm values of dice score, Jaccard index, and Hausdorff distance (HD)

Models	Dice score	Jaccard index	HD
23 layers CNN	0.63	0.66	2.12
Ensemble model	0.69	0.68	1.98
Fractional	0.72	0.71	1.86
PCA and TK- means	0.75	0.76	1.79
Proposed algorithm	0.78	0.88	1.72

The assessment of brain tumor detection in MRI images has been conducted utilizing three metrics, specifically the Dice score, Jaccard index, and Hausdorff distance. Jaccard index and Dice coefficient are measures of similarity between the sets of pixels. The dice score varies between the range 0 and 1, with 1 representing the closest match between forecasted and actual values. The higher the Dice score and Jaccard index, the better the performance of the model. A model's performance improves as the Dice score and Jaccard index increase. Conversely, the HD is an important criterion as it provides valuable information about the largest segmentation error. HD calculates the distance between the non-zero pixels of two images using the formula specified in Eq. (16). The lower the Hausdorff distance, the better the performance of the model. Compared to the existing models depicted in **Table 5**, the 23 layers CNN and Ensemble model had lower Dice scores, Jaccard index, and low Hausdorff distances. This indicates that the proposed algorithm has improved the accuracy of brain tumor detection

when compared to these models. The Fractional wavelet [31] and PCA and TK-means [28] models had better Dice scores and Jaccard index than the 23 layers CNN [29] and Ensemble model [32], but they had higher Hausdorff distances. This suggests that these models were better at predicting the location of the tumor, but not the boundary.

Overall, the proposed algorithm shows promising results in detecting brain tumors in MRI images when compared to the existing models. However, further improvements are needed to reduce the variability in detecting the distance between the predicted and ground truth tumor boundaries as indicated by the higher Hausdorff distance.

5.2 Impact of Accuracy Level

The performance accuracy level is computed based on the true positives and true negatives to identify the normal as well as abnormal MRI images. As illustrated in the graph, the performance of accuracy level is found to be increased using the proposed ACNN. One of the crucial parts of neural networks is the loss function, which measures model prediction error. The model has been trained with the help of training data.

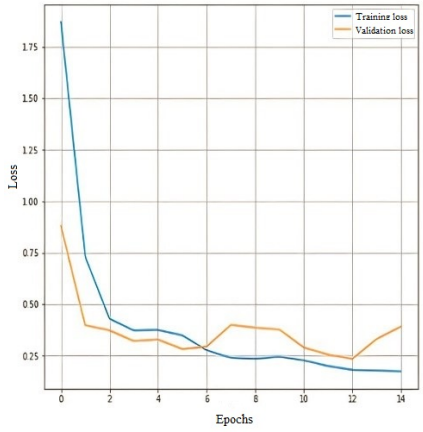

(a)

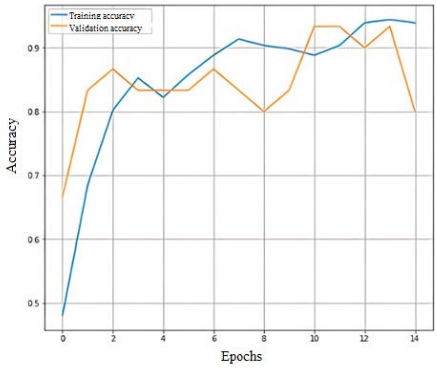

(b)

Fig. 6. Measurement Analysis of training and validation (a) Loss (b) accuracy

Additionally, validation loss is employed to evaluate how well a deep learning strategy performs on the validation set for brain image categorization. **Fig. 6** (a) model training and validation loss and (b) training and validation accuracy for epochs =14 on the training and validation data. At epoch 14, the training loss is 0.23, and the validation loss value is 0.43. The suggested ACNN pre-processes the MRI images to eliminate noise employing a KB filter, and this significantly demonstrates that the accuracy is higher and the identification seems more reliable. The training accuracy value is 1.0, while the validation accuracy value is 0.8. Also, the Adam optimizer in addition helps the model for optimizing the neural networks during training.

5.3 Impact of Precision and Recall

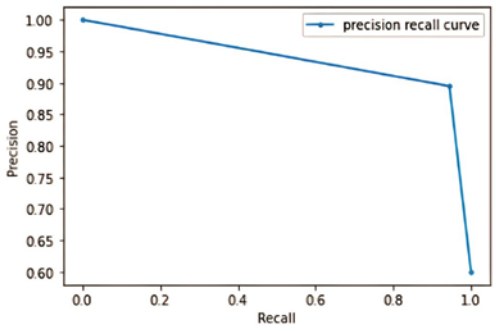

Fig. 7. Measurement of Precision-Recall

The precision-recall curve (PRC), which depicts the connection between precision as well as recall, has numerous uses in the area of categorization. The recall on the horizontal axis displays the properly anticipated ratio of positive samples to genuine samples, whereas the precision values on the vertical axis show the right predictions as the ratio of positive samples to all positive samples. A high level of recall and precision indicates strong categorization ability. Based on several accuracy metrics and the ROC curve, the suggested work performs exceptionally well in binary-class categorization, as shown in **Fig. 7**. The noisy pixels are eliminated through image tissue pre-processing, and image tissue segmentation divides the image into several sections. Then, image tissue feature extraction is performed to extract the features, resulting in image classification with higher precision and recall. The graph in **Fig. 7**, to a moderate extent, bows towards (1, 1), indicating a decently trained model.

5.4 Impact of Mean Absolute Error

The percentage of patient data that are mistakenly identified as being sick or not depends on the Mean Absolute Error (MAE). The mean absolute error is formulated as,

$$MAE = \left(\frac{PD_{fp}+PD_{fn}}{N}\right) * 100 \tag{17}$$

From (17), 'MAE' denotes the mean absolute error. 'PD_{fp}' denotes the false positive. 'PD_{fn}' symbolizes the false negative. 'N' symbolizes the number of MR Images. MAE is expressed as a percentage (%). **Fig. 8** shows the mean absolute error as a graphical depiction.

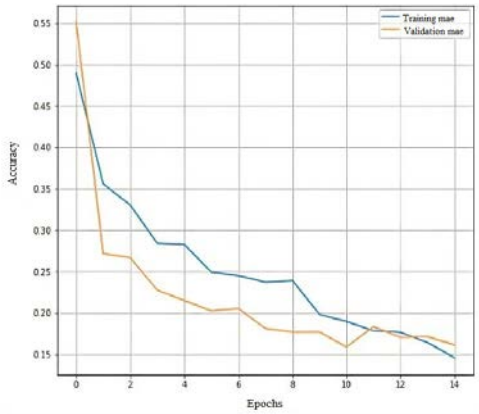

(a)

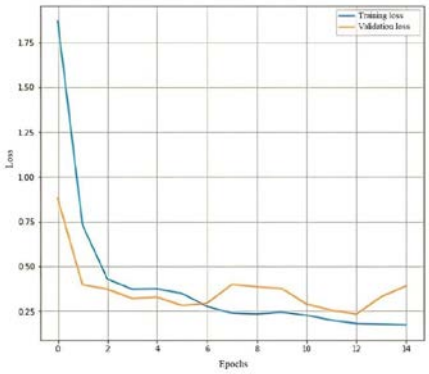

(b)

Fig. 8. Measurement Analysis of Mean Absolute Error (a) accuracy (b) loss

The performance of mean absolute error using three methods is computed based on false positives and false negatives. The proposed model shows promising results based on the MAE value of loss and accuracy. The training process of the model lasted for 14 epochs, during which the training loss and validation loss were recorded as 0.25 and 0.42, respectively. This suggests that the model was able to reduce the loss during the training process, indicating that it learned the patterns in the data effectively.

Furthermore, the MAE (Mean Absolute Error) scores for training and validation were 0.15 and 0.18, respectively. The model's effectiveness tends to increase as the MAE values decrease. The fact that the validation MAE value is low indicates that the model is not overfitting the training set. Consequently, it can be inferred that the model accurately predicted the presence or absence of brain tumors in the given MRI scans.

5.5 Impact of receiver operating characteristic curve

In a graphical technique, the Receiver Operating Characteristic curve is abbreviated as ROC for displaying the tradeoff between the false positive rate of a deep learning classifier and the true positive rate of a learning deep classifier.

The ROC curve is illustrated in **Fig. 9** using the true positive rate and the false positive rate. The curve closer to the upper left corner indicates that the proposed approach accurately classifies tumors from MRI scan images with a value of 0.98 in the proposed ACNN. ROC curve is determined through pre-processing, segmentation, and feature extraction for image classification with brain tumors. At first, the noisy pixels are removed by image tissue pre-processing using the KB filter and then, the pre-processed image is divided into several segments using isotonic regression. Lastly, the features extracted using the Marr wavelet detect and localizes the tumor efficiently with a fast computation time and also it can handle large dataset.

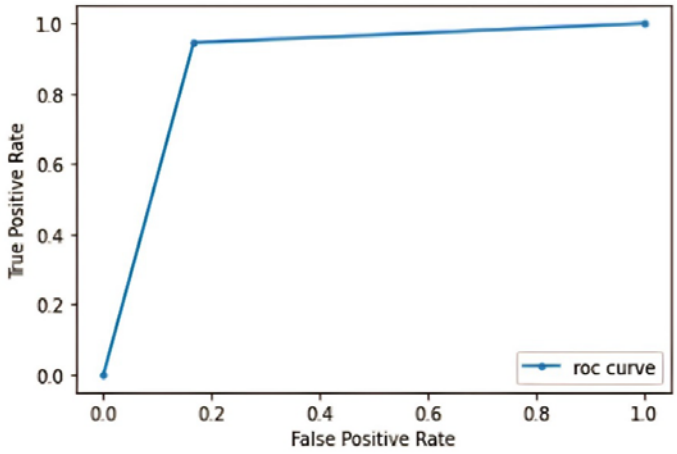

Fig. 9. Measurement Analysis of ROC curve

5.6 K-fold validation

The k-fold technique is a popular validation method where the training dataset is divided into k-folds, known as cross-validation. One fold is used for testing while the remaining k-1 folds are used for training, and this process is repeated for each fold. The results are evaluated collectively, and the mean accuracy is calculated. While this technique works well for balanced classification problems, it is not effective for imbalanced classes since it randomly divides the data without considering class imbalance. To address this, the stratified k-fold cross-validation technique is used, which maintains the same class ratio throughout the folds. Common values for k are 3, 5, and 10. In this study, a value of 10 was chosen to maximize classification accuracy. The K-fold cross-validation based on training and testing samples has been evaluated to determine the robustness of the proposed model. The accuracy, precision, recall, and F1-score for a 10-fold cross-validation based on the proposed ACNN model is shown in **Fig. 10(a)**, **Fig. 10(b)**, **Fig. 10(c)**, and **Fig. 10(d)** respectively.

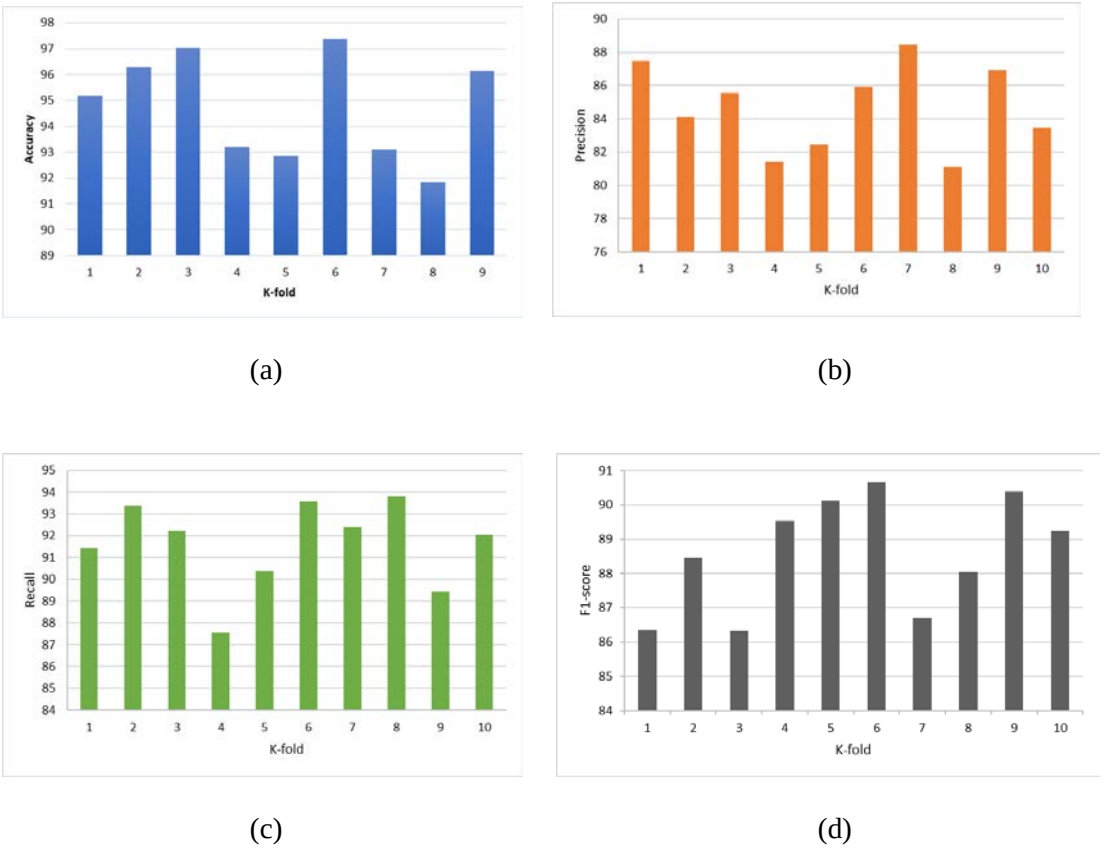

(a) (b)

(c) (d)

Fig. 10. Measurement Analysis of ROC curve

The proposed ACNN model was evaluated using k-fold cross-validation, and its performance was assessed using various metrics. Firstly, accuracy was used to measure the overall correctness of the model's predictions. The ACNN model achieved an average accuracy of 94.95% across the ten folds, with accuracy values ranging from 91.84% (fold 5) to 97.39% (fold 6). This consistently high accuracy suggests that the ACNN model excels at correctly classifying instances from the dataset. Next, precision was examined, which represents the proportion of correctly predicted positive instances (tumor) out of the total instances predicted as positive. The ACNN model achieved an average precision of 84.97% across the ten folds, with precision values ranging from 81.11% (fold 8) to 88.42% (fold 7). These results indicate that the model exhibits reasonably good precision, showcasing its ability to minimize false positives.

Also, the ACNN model achieved an average recall of 91.64% across the ten folds, with recall values ranging from 87.56% (fold 4) to 93.56% (fold 6). These high recall values suggest that the ACNN model is effective in identifying the majority of positive instances. The F1-score, which combines precision and recall into a single metric, was also considered. The ACNN model achieved an average F1-score of 88.95% across the ten folds, with F1-score values ranging from 86.32% (fold 3) to 90.67% (fold 6). The consistent F1-score values indicate that the model can strike a good balance between precision and recall.

Overall, the evaluation of the proposed ACNN model using k-fold cross-validation demonstrates its strong performance in terms of accuracy, precision, recall, and F1 score.

These metrics provide a comprehensive assessment of the model's predictive capabilities. The consistently high performance across the ten folds indicates the model's robustness and potential for practical applications.

6. Conclusion

The ACNN model provides a promising approach for enhancing the accuracy of brain tumor detection from MR images. The model leverages a combination of advanced techniques including KB Denoising, Isotonic Regressive Image Tissue Segmentation, and Marr Wavelet Transformation-based feature extraction, coupled with CNN architecture. The results of the experiments revealed that the proposed model outperformed traditional methods in terms of various evaluation metrics. These metrics included accuracy, sensitivity, precision, dice score, Jaccard index, Positive predictive value, recall, Hausdorff distance, specificity, and F1 score. According to the experimental results, a proposed ACNN attained a maximum accuracy of 98.8% which is higher than the other existing models. Hence, the ACNN model has the potential to serve as a valuable resource for assisting healthcare practitioners in the timely identification and diagnosis of brain tumors, thereby potentially enhancing patient outcomes and survival rates. However, one limitation of the proposed method is its reliance on a substantial volume of training data, which can pose challenges and consume considerable time. To overcome these limitations in the future, alternative deep learning architectures will be explored that require fewer data for training and validation. Additionally, the model can be further optimized by incorporating additional features or imaging modalities to improve its performance.

Acknowledgment

The author would like to appreciate the effort of the editors and reviewers. This research did not receive any specific grant from funding agencies in the public, commercial, or not-for-profit sectors.

References

[1] K. S. Ananda Kumar, A. Y. Prasad, and J. Metan, "A hybrid deep CNN-Cov-19-Res-Net Transfer learning archetype for an enhanced Brain tumor Detection and Classification scheme in medical image processing," *Biomed. Signal Process. Control*, vol. 76, p. 103631, Jul. 2022. Article (CrossRef Link)

[2] S. Abirami and D. G. K. D. Prasanna Venkatesan, “Deep learning and spark architecture based intelligent brain tumor MRI image severity classification,” *Biomed. Signal Process. Control*, vol. 76, p. 103644, Jul. 2022. Article (CrossRef Link)

[3] N. Bhagat and G. Kaur, “MRI brain tumor image classification with support vector machine,” *Mater. Today*, vol. 51, pp. 2233–2244, Mar. 2022. Article (CrossRef Link)

[4] S. Ahuja, B. K. Panigrahi, and T. K. Gandhi, “Enhanced performance of Dark-Nets for brain tumor classification and segmentation using colormap-based superpixel techniques,” *Machine Learning with Applications*, vol. 7, p. 100212, Mar. 2022. Article (CrossRef Link)

[5] G. Neelima, D. R. Chigurukota, B. Maram, and B. Girirajan, “Optimal DeepMRSeg based tumor segmentation with GAN for brain tumor classification,” *Biomed. Signal Process. Control*, vol. 74, p. 103537, Apr. 2022. Article (CrossRef Link)

[6] D. Kapila and N. Bhagat, “Efficient feature selection technique for brain tumor classification utilizing hybrid fruit fly based abc and ann algorithm,” *Mater. Today*, vol. 51, pp. 12–20, Apr. 2022. Article (CrossRef Link)
[7] V. Sabitha, J. Nayak, and P. R. Reddy, “WITHDRAWN: MRI brain tumor detection and classification using KPCA and KSVM,” *Mater. Today*, Mar.2021. Article (CrossRef Link)
[8] C. Öksüz, O. Urhan, and M. K. Güllü, “Brain tumor classification using the fused features extracted from expanded tumor region,” *Biomed. Signal Process. Control*, vol. 72, p. 103356, Feb. 2022. Article (CrossRef Link)
[9] B. Srikanth and S. Venkata Suryanarayana, "WITHDRAWN: Multi-Class classification of brain tumor images using data augmentation with a deep neural network," *Mater. Today*, Mar. 2021. Article (CrossRef Link)
[10] P. Harish and S. Baskar, “WITHDRAWN: MRI based detection and classification of brain tumor using enhanced faster R-CNN and Alex Net model,” *Mater. Today*, Dec. 2020. Article (CrossRef Link)
[11] A. S. M. Shafi, M. B. Rahman, T. Anwar, R. S. Halder, and H. M. E. Kays, “Classification of brain tumors and auto-immune disease using ensemble learning,” *Inform. Med. Unlocked*, vol. 24, p. 100608, May.2021. Article (CrossRef Link)
[12] R. Mehrotra, M. A. Ansari, R. Agrawal, and R. S. Anand, "A Transfer Learning Approach for AI-based classification of brain tumors," *Machine Learning with Applications*, vol. 2, p. 100003, Dec. 2020. Article (CrossRef Link)
[13] T. Sathies Kumar, C. Arun, and P. Ezhumalai, “An approach for brain tumor detection using optimal feature selection and optimized deep belief network,” *Biomed. Signal Process. Control*, vol. 73, p. 103440, Mar. 2022. Article (CrossRef Link)
[14] J. Amin, M. Sharif, M. Yasmin, and S. L. Fernandes, “A distinctive approach in brain tumor detection and classification using MRI,” *Pattern Recognit. Lett.*, vol. 139, pp. 118–127, Nov.2020. Article (CrossRef Link)
[15] P. M. Siva Raja and A. V. Rani, “Brain tumor classification using a hybrid deep autoencoder with Bayesian fuzzy clustering-based segmentation approach,” *Biocybern. Biomed. Eng.*, vol. 40, no. 1, pp. 440–453, Mar. 2020. Article (CrossRef Link)
[16] A. Chattopadhyay and M. Maitra, “MRI-based brain tumor image detection using CNN-based deep learning method," *Neuroscience Informatics*, vol. 2, no. 4, p. 100060, Dec. 2022. Article (CrossRef Link)
[17] G. S. Tandel, A. Balestrieri, T. Jujaray, N. N. Khanna, L. Saba, and J. S. Suri, “Multiclass magnetic resonance imaging brain tumor classification using artificial intelligence paradigm,” *Comput. Biol. Med.*, vol. 122, p. 103804, Dec. 2020. Article (CrossRef Link)
[18] P. Tiwari, B. Pant, M. M. Elarabawy, M. Abd-Elnaby, N. Mohd, G. Dhiman, and S. Sharma, “CNN based multiclass brain tumor detection using medical imaging,” *Comput. Intell. Neurosci.*, vol. 2022, p. 1830010, Jun. 2022. Article (CrossRef Link)
[19] H. Alsaif, R. Guesmi, B. M. Alshammari, T. Hamrouni, T. Guesmi, A. Alzamil, and L. Belguesmi, “A novel Data Augmentation-based brain tumor detection using convolutional neural network,” *Appl. Sci. (Basel)*, vol. 12, no. 8, p. 3773, Apr. 2022. Article (CrossRef Link)
[20] M. Jian, X. Zhang, L. Ma, and H. Yu, “Tumor detection in MRI brain images based on saliency computational modeling,” *IFAC-PapersOnLine*, vol. 53, no. 5, pp. 43–46, May. 2020. Article (CrossRef Link)
[21] D. Pavani, K. Durgalaxmi, B. S. Datta, and D. Nagajyothi, “Brain tumor detection using convolutional neural networks in MRI images,” in *Proc. of Int. Conf. on. Soft Comput & Signal Proc*, pp. 751-760, 2022. Article (CrossRef Link)
[22] S. K. Mishra and V. H. Deepthi, “RETRACTED ARTICLE: Brain image classification by the combination of different wavelet transforms and support vector machine classification,” *J. Ambient Intell. Human. Comput.*, vol. 12, no. 6, pp. 6741-6749, Jun. 2021. Article (CrossRef Link)

[23] T. Han-Trong, H. Nguyen Van, H. Nguyen Thi Thanh, V. Tran Anh, D. Nguyen Tuan, and L. Vu Dang, "An efficient method for diagnosing brain tumors based on MRI images using Deep Convolutional Neural Networks," *Appl. Comput. Intell. Soft Comput.*, vol. 2022, pp. 1–18, Mar 2022. Article (CrossRef Link)
[24] M. Arif, F. Ajesh, S. Shamsudheen, O. Geman, D. Izdrui, and D. Vicoveanu, "Brain tumor detection and classification by MRI using biologically inspired orthogonal wavelet transform and deep learning techniques," *J. Healthc. Eng.*, vol. 2022, p. 2693621, Jan. 2022. Article (CrossRef Link)
[25] A. Ali, H.A Rahim, M.F. Pasha, R. Dowsley, M. Masud, J. Ali, and M. Baz, "Security, Privacy, and Reliability in Digital Healthcare Systems Using Blockchain," *Electronics*, vol. 10, no. 16, p. 2034, Aug. 2021. Article (CrossRef Link)
[26] A. Ali, M. A. Almaiah, F. Hajjej, M.F. Pasha, O.H. Fang, R. Khan, J. Teo, and M. Zakarya, "An industrial IoT-based blockchain-enabled secure searchable encryption approach for healthcare systems using neural network," *Sensors (Basel)*, vol. 22, no. 2, p. 572, Jan. 2022. Article (CrossRef Link)
[27] M. A. Almaiah, F. Hajjej, A. Ali, M. F. Pasha, and O. Almomani, "A novel hybrid trustworthy decentralized authentication and data preservation model for digital healthcare IoT based CPS," *Sensors (Basel)*, vol. 22, no. 4, p. 1448, Feb. 2022. Article (CrossRef Link)
[28] M. K. Islam, M. S. Ali, M. S. Miah, M. M. Rahman, M. S. Alam, and M. A. Hossain, "Brain tumor detection in MR image using superpixels, principal component analysis and template based K-means clustering algorithm," *Mach. Learn. Appl.*, vol. 5, p. 100044, Sep. 2021. Article (CrossRef Link)
[29] M. S. I. Khan et al., "Accurate brain tumor detection using deep convolutional neural network," *Comput. Struct. Biotechnol. J.*, vol. 20, pp. 4733–4745, Aug. 2022. Article (CrossRef Link)
[30] O. Patil and S. T. Hamde, "Automated detection of brain tumor disease using empirical wavelet transform based LBP variants and ant-lion optimization," *Multimed. Tools Appl.*, vol. 80, no. 12, pp. 17955–17982, Feb. 2021. Article (CrossRef Link)
[31] B. Kaushal, M.D. Patil, and G. K. Birajdar, "Fractional wavelet transform based diagnostic system for brain tumor detection in MR imaging," *Int. J. Imaging Syst. Technol.*, vol. 31, no. 2, pp. 575-591, 2021. Article (CrossRef Link)
[32] O. Turk, D. Ozhan, E. Acar, T. C. Akinci, and M. Yilmaz, "Automatic detection of brain tumors with the aid of ensemble deep learning architectures and class activation map indicators by employing magnetic resonance images," *Z. Med. Phys.*, Dec. 2022. Article (CrossRef Link)
[33] El Khayaty, T., "BrainTumor_ImageData_Classification&Segmentation [Data set]," 2022. Article (CrossRef Link)

M. MohanaSundari is currently working at Velalar College of Engineering and Technology in the Department of Computer Science and Engineering as an Assistant Professor, with 12 years of experience. Her areas of interest include Networks, Image Processing, Deep Learning, and Machine Learning. She has authored more than 10 papers in reputable journals and has actively participated in various Faculty Development Programs (FDPs), seminars, and workshops on emerging technologies. Additionally, she has presented more than 15 papers at both national and international conferences.

Dr. V. Chandrasekaran is currently employed at Velalar College of Engineering and Technology in the Department of Electronics and Communication Engineering as a Professor, with 17 years of experience. His areas of interest include Networks, Image Processing, and Machine Learning. He has published over 10 papers in reputable journals and has participated in various Faculty Development Programs (FDPs), seminars, and workshops on emerging technologies. Additionally, he has organized numerous funding seminars and workshops and has presented more than 15 papers at both national and international conferences.

Dr. S. Anitha is currently employed at Kongu Engineering College in the Department of Information Technology, where she has served as an Assistant Professor for 17 years. Her primary areas of interest include Networks, Wireless Sensor Networks, and Machine Learning. She has an impressive track record of publishing over 20 papers in reputable journals and actively participating in various FDP, seminars, and workshops focusing on emerging technology. Her work has garnered over 100 citations in scholarly journals. Additionally, she has served as a resource person for numerous FDPs and workshops and has organized various successful funding seminars. She has also presented more than 25 papers at both national and international conferences.